Earthline Journal of Chemical Sciences
E-ISSN: 2581-9003; CODEN: EJCSB4
Volume 11, Number 1, 2024, Pages 83-103
https://doi.org/10.34198/ejcs.11124.083103

Ladder-like Organostannoxane: Synthesis and Crystal Structure of the Second Polymorph $\{[(C_6H_5)_2Sn]_2[(C_6H_5)_2ClSn]_2(\mu_3\text{-}O)_2(\mu_2\text{-}OH)_2\}\cdot[DMF]_2$

Modou Sarr[1], Mouhamadou Birame Diop[1,*], Mouhamadou Sembene Boye[1,2], Aminata Diassé-Sarr[1], Libasse Diop[1] and Allen G. Oliver[3]

[1] Laboratoire de Chimie Minérale et Analytique, Département de Chimie, Faculté des Sciences et Techniques, Université Cheikh Anta Diop, Dakar, Sénégal

[2] Département de Physique-Chimie, Faculté des Sciences et Technologies de l'Education et de la Formation (FASTEF), Université Cheikh Anta Diop, Dakar, Sénégal

[3] Department of Chemistry and Biochemistry, University of Notre Dame, Nieuwland, Science Hall, Notre Dame, USA

[*] Corresponding author e-mail: mouhamadoubdiop@gmail.com

Abstract

A ladder-like organostannoxane identified as a polymorph of bis-[chloro-(μ_2-hydroxo)-(μ_3-oxo)-tetraphenyl-di-tin] dimethylformamide solvate, $\{[(C_6H_5)_2Sn]_2[(C_6H_5)_2ClSn]_2(\mu_3\text{-}O)_2(\mu_2\text{-}OH)_2\}\cdot[DMF]_2$ (**1**), has been synthesized and structurally characterized by means of single-crystal X-ray diffraction analysis. Compound **1** crystallizes in the monoclinic space group $P2_1/c$ with a = 23.4137(12) Å, b = 11.2525(6) Å, c = 20.2719(11) Å, β = 100.461(2)°, V = 5252.1(5) Å^3, Z = 4 and Z' = 1. The XRD discloses that the polymorph reported in this work is the full molecule which does not crystallize about any inversion center. Complex **1** exhibits a tetranuclear organotin(IV) ladder-like structure containing two external chlorides. The tetranuclear structure is comprised of a three-rung-staircase Sn_4O_4 cluster which consists of a ladder of four Sn_2O_2 units. The central Sn_2O_2 core forms dihedral angles of 4.00(7)° and 1.62(8)° with its two fused four-membered rings, describing a slightly bent ladder. This folding is further noticed with the dihedral angle between the two external Sn_2O_2 cores of 4.65(8)°. In the structure, two types of distorted trigonal bipyramid geometry at tin centers like-arrangement are disclosed. The most Sn–O bridges bond lengths describe a static *trans* effect affording dissymmetrical bonds. The dimethylformamide solvate molecules form a dihedral angle of 74.5(2)° and are interlinked to the tetranuclear organotin(IV) ladder *via* O–H···O hydrogen bond patterns.

Received: October 12, 2023; Accepted: November 14, 2023; Published: November 21, 2023

Keywords and phrases: organostannoxane; tetranuclear organotin(IV) ladder; trigonal bipyramid; crystal structure; polymorph.

Additional inner C–H···Cl and C–H···O hydrogen bonds as well the C–H···O interactions are present. Moreover, the intermolecular C–H···O hydrogen bonds do not contribute to direct the crystal structure framework; they do not play an important function in forming a supramolecular architecture.

1. Introduction

Coordination polymers, isolated from an appropriate reaction of selected metal centers and multidirectional ligands, aroused an intriguing interest to researchers due to the potential applications as well the fascinating structures they display [1-9]. Organotin(IV) carboxylate based complexes and derivatives have been widely investigated because they are a class of compounds affording very interesting topologies, and a variety of structural types such tetramers and oligomeric ladders [10-12]. The organostannoxanes in particular, attracted an incommensurable interest because of the diverse structures they exhibit [13-16]. Several tetranuclear compounds with an inversion center (Z'=0.5) $\{[(C_6H_5)_2Sn]_2[(C_6H_5)_2ClSn]_2(\mu_3\text{-}O)_2(\mu_2\text{-}OH)_2\}$ [17-19], $\{[(C_6H_5)_2Sn]_2[(C_6H_5)_2ClSn]_2(\mu_3\text{-}O)_2(\mu_2\text{-}OCH_3)_2\}$ [20], $\{[(C_6H_5)_2Sn]_2[(C_6H_5)_2BrSn]_2(\mu_3\text{-}O)_2(\mu_2\text{-}OH)_2\}$ [21], $\{[(i\text{-}C_3H_7)_2Sn]_2[(i\text{-}C_3H_7)_2ClSn]_2(\mu_3\text{-}O)_2(\mu_2\text{-}OH)_2\}$ [22], $\{[(CH_2C_6H_4Cl)_2Sn]_2[(CH_2C_6H_4Cl)_2ClSn]_2(\mu_3\text{-}O)_2(\mu_2\text{-}OH)_2\}$ [23], $\{[(C_2H_5)_2Sn]_2[(C_2H_5)_2ClSn]_2(\mu_3\text{-}O)_2(\mu_2\text{-}OH)_2\}$ [24], $\{[(CH_2C_6H_4CH_3)_2Sn]_2[(CH_2C_6H_4CH_3)_2ClSn]_2(\mu_3\text{-}O)_2(\mu_2\text{-}OH)_2\}$ [25], and $\{[(CH_2C_6H_5)_2Sn]_2[(CH_2C_6H_5)_2ClSn]_2(\mu_3\text{-}O)_2(\mu_2\text{-}OH)_2\}$ [26], or without an inversion center (Z'=1) $\{[(C_6H_{11})_2Sn]_2[(t\text{-}C_4H_9)_2ClSn]_2(\mu_3\text{-}O)_2(\mu_2\text{-}OH)_2\}$ [27], and $\{[(CH_2Si(CH_3)_3)_2Sn]_2[(CH_2Si(CH_3)_3)_2ClSn]_2(\mu_3\text{-}O)_2(\mu_2\text{-}OH)_2\}$ [22], describing crystal structures containing a ladder based structural motif were previously isolated. The first polymorph of bis-[chloro-(μ_2-hydroxo)-(μ_3-oxo)-tetraphenyl-di-tin] dimethylformamide solvate has been investigated by single crystal X-ray diffraction analysis based on a 80% data collection achieved at 293 K due to the lack of stability of the used sample [28]. Very few compounds closely related to bis-[chloro-(μ_2-hydroxo)-(μ_3-oxo)-tetraphenyl-di-tin] ladder, comprising solvate molecules were otherwise investigated [29-32]. Since decades, the Dakar group has been involved in the investigation of new organotin(IV) based materials [33-38], and more recently, singularly in ladder-like organostannoxanes derived from carboxylic acid [10]. In our course of isolating and investigating new organotin(IV) hybrid materials, we report in this work the synthesis and crystal characterization of the second polymorph organostannoxane, $\{[(C_6H_5)_2Sn]_2[(C_6H_5)_2ClSn]_2(\mu_3\text{-}O)_2(\mu_2\text{-}OH)_2\}\cdot[DMF]_2$ (**1**).

2. Materials and Methods

2.1. General

Reagents monocyclohexylamine, $[(C_6H_{11})NH_2]$ (99 % purity), benzoic acid, $C_6H_5CO_2H$ (99 % purity), and diphenyltin dichloride, $Sn(C_6H_5)_2Cl_2$ (96 % purity) were purchased from Sigma-Aldrich, Steinheim am Albuch, Germany and were used without any further purification. The X-ray crystallographic data for compound **1** were collected using a Bruker APEX-II diffractometer.

2.2. Synthesis and isolation

The isolation of the second polymorph investigated in this work follows a two steps. Preliminary, monocyclohexylamine was mixed with benzoic acid in water yielding a white powder, presumably $[C_6H_{11}NH_3][(C_6H_5CO_2]$ (**L_1**). A 15mL methanolic solution of the presumable ligand **L_1** (99 mg; 0.45 mmol), and a 15mL dimethylformamide solution of $Sn(C_6H_5)_2Cl_2$ (154.7 mg; 0.45 mmol) were mixed and the clear obtained mixture stirred at room temperature (303 K) for 2 h. After several days of slow evaporation, colorless block-like crystals suitable for single-crystal X-ray structure determination were collected from the supernatant solution.

2.3. Single crystal diffraction

A crystal of approximate dimensions 0.137×0.119×0.09 mm was used for data collection. The X-ray crystallographic data was collected using a Bruker Kappa X8-APEX-II at T = 120(2) K. Data was measured using ωand φ scans using Mo$K\alpha$ radiation (λ = 0.71073 Å) using a collection strategy to obtain a hemisphere of unique data determined by *Apex3* [39]. Cell parameters were determined and refined using the program *SAINT* [40]. Data were corrected for absorption, polarization and other effects using intensity measurements by *SADABS* [41]. The structure was solved by *SHELXT* [42] and refined using least-squares minimization with *SHELXL* [43].

Program used for the representation of the molecular and crystal structures: *Olex2* [44]. Crystal data, data collection and structure refinement details for compound **1** are summarized in Table **1**. Selected angles and bond lengths for the polymorph **1** are listed in Tables **2**-**4**.

CCDC 2300931 (**1**) contains the supplementary crystallographic data for this paper. Copies of these data can be obtained free of charge from the Cambridge Crystallographic Data Centre (CCDC), 12 Union Road, Cambridge CB2 1EZ, UK (fax: int. Code +44 1223 336 033; e-mail: deposit@ccdc.cam.ac.ukor www: http://www.ccdc.cam.ac.uk).

Table 1. Crystal data and structure refinement for **1**.

Parameters	**1**
Empirical formula	$C_{54}H_{56}N_2O_6Cl_2Sn_4$
Formula weight	1374.66
Temperature/K	120(2)
Crystal system	Monoclinic
Space group	$P2_1/c$
a/Å	23.4137(12)
b/Å	11.2525(6)
c/Å	20.2719(11)
α/°	90
β/°	100.461(2)
γ/°	90
Volume/Å^3	5252.1(5)
Z/Z'	4/1
ρ_{calc}g/cm^3	1.738
μ/mm^{-1}	2.032
F(000)	2704
Crystal size/mm^3	0.137 × 0.119 × 0.09
Radiation	MoKα (λ = 0.71073)
2Θ range for data collection/°	3.538 to 56.932
Index ranges	$-30 \leq h \leq 31$ $-15 \leq k \leq 15$ $-27 \leq l \leq 27$
Reflections collected	116849
Independent reflections	13232[R_{int} =0.0472;R_{sigma} = 0.0275]

Parameters	**1**
Data/restraints/parameters	13232/0/619
Goodness-of-fit on F^2	1.032
Final R indexes [I>=2σ (I)]	R_1 = 0.0246
	wR_2 = 0.0466
Final R indexes [all data]	R_1 = 0.0428
	wR_2 = 0.0520
Largest diff. peak/hole / e Å^{-3}	0.73/-0.69

R1 = $\Sigma(||F_o|-|F_c||)/\Sigma|F_o|$; wR2 = $[\Sigma w(F_o^2-F_c^2)^2/\Sigma[w(F_o^2)^2]^{1/2}$ where w = $1/[\sigma^2(F_o^2)$ + $(0.0174P)^2$ + 4.1130P] where P = $(F_o^2)+2F_c^2)/3$; [c] goodness of fit = $[\Sigma w(F_o^2-F_c^2)^2/(N_o-N_v)]^{1/2}$.

3. Results and Discussion

Compound **1** was isolated from the reaction of a 1:1 molar ratio of a dimethylformamide solution of $Sn(C_6H_5)_2Cl_2$, and a methanol solution of the reaction product between equimolar aqueous solutions of cyclohexyl amine and benzoic acid. Colorless single crystals grew from the solution (Eq. 1) and have been characterized as **1**, $\{[(C_6H_5)_2Sn]_2[(C_6H_5)_2ClSn]_2(\mu_3\text{-}O)_2(\mu_2\text{-}OH)_2\}\cdot[DMF]_2$. The tetranuclear ladder is obtained from a hydrolysis reaction of $Sn(C_6H_5)_2Cl_2$. To our knowledge, only three examples of crystal structures involving this tetranuclear component co-crystallized with organic solvents *viz* dimethylformamide [28], acetone [31], and dimethylsulfoxide [32].

$$4\ Sn(C_6H_5)_2Cl_2 + 4\ H_2O + 2\ DMF \xrightarrow[CH_3C(O)CH_3]{(C_6H_{11}NH_3)(C_6H_5CO_2)} \{[(C_6H_5)_2Sn]_2[(C_6H_5)_2ClSn]_2(\mu_3\text{-}O)_2(\mu_2\text{-}OH)_2\}\cdot[DMF]_2 + 6\ HCl \quad (1)$$

The polymorph **1** does not crystallize about the inversion center contrary to the known first polymorph reported by Tiekink [28] which crystallizes about the inversion center at [0, 0, 0.5] disclosing that only half of the molecule is observed in the asymmetric unit. The molecule described herein is the full. In Figure 1 is illustrated a perspective view of the asymmetric unit of compound **1**.

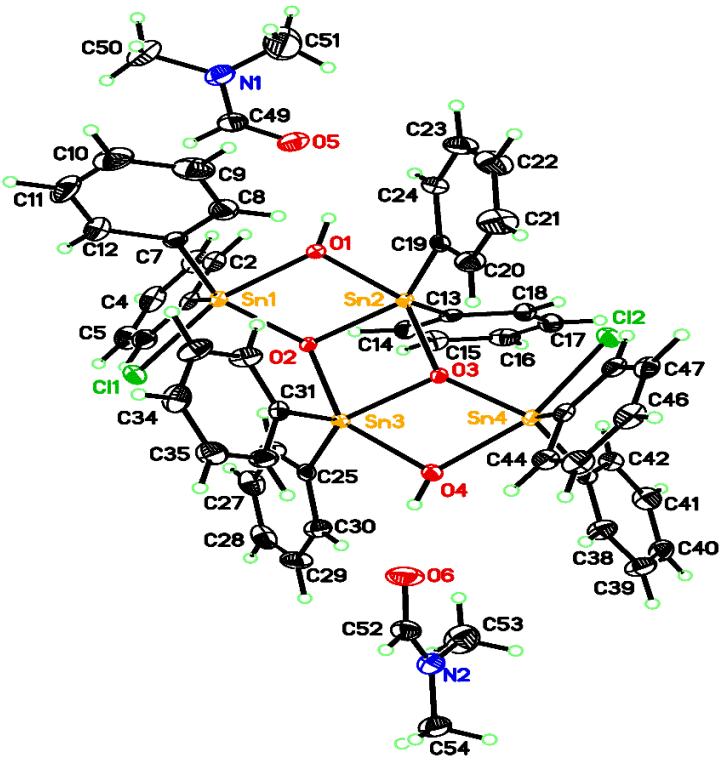

Figure 1. The asymmetric unit of **1** showing 50% probability ellipsoids for atoms and the crystallographic numbering scheme adopted.

The structure is comprised of the hydroxide-bridged tetrameric organostannoxane ladder-like structure including two exogenous chlorides and two DMF solvate molecules. The ladder-like structure described in **1** consists of the $Sn_4(\mu_3\text{-}O)_2(\mu_2\text{-}OH)_2$ moiety and the two chlorides. Similarly to other encountered tetrameric organostannoxanes [10, 28-32], the molecular structure is based on a centrosymmetric Sn_2O_2 core linked to two exocyclic tin centers through the triply bridging oxygen μ_3-O atoms. In addition to the triply bridging μ_3-O atoms which connect the pair of exocyclic tin centers to the central Sn_2O_2 unit, hydroxide μ_2-O atoms also bridge these aforesaid groups. The sums of the angles about the triply bridged μ_3-O atoms, whose three electron pairs are shared with three Sn(IV) atoms, of 359.46° (O2) and 359.95° (O3) (see Table 2 for details) evidence, instead of the expected trigonal pyramidal fashions because bearing one free pair of electrons according to the Gillespie-Nyholm theory (Valence Shell Electron Pair

Repulsion, VSEPR), a planarity about μ_3-O owing to a strong throttling within the Sn_4O_4 cluster. This trigonal planar geometry about μ_3-O is confirmed by the O2Sn1Sn2Sn3 and O3Sn2Sn3Sn4 planes' r.m.s deviation values of 0.036 Å and 0.010 Å, respectively.

Table 2. Selected angle values (°) at μ_3-O and μ_2-O atoms for polymorph **1**.

Atom-atom-atom	Angle value	Atom-atom-atom	Angle value
μ_3-O		μ_3-O	
Sn1–O2–Sn2	110.41 (7)	Sn2–O1–Sn1	102.59 (7)
Sn1–O2–Sn3	143.00 (8)	Sn2–O1–H1	109.5
Sn2–O2–Sn3	106.05 (7)	Sn1–O1–H1	137.4
Sn4–O3–Sn3	110.72 (7)	Sn3–O4–Sn4	102.71 (7)
Sn4–O3–Sn2	143.19 (8)	Sn3–O4–H4	109.5
Sn3–O3–Sn2	106.04 (7)	Sn4–O4–H4	147.8

Table 3. Selected angle values (°) at Sn(IV) atoms for polymorph **1**.

Atom-atom-atom	Angle value	Atom-atom-atom	Angle value
O2–Sn1–C7	115.85 (8)	O2–Sn2–C13	112.39 (8)
O2–Sn1–C1	118.58 (8)	O2–Sn2–C19	117.36 (8)
C7–Sn1–C1	124.42 (10)	C13–Sn2–C19	130.15 (9)
O2–Sn1–O1	73.38 (6)	O2–Sn2–O1	73.35 (6)
C7–Sn1–O1	93.46 (8)	C13–Sn2–O1	95.47 (8)
C1–Sn1–O1	91.58 (8)	C19–Sn2–O1	95.61 (8)
O2–Sn1–Cl1	89.01 (5)	O2–Sn2–O3	74.01 (6)
C7–Sn1–Cl1	95.10 (7)	C13–Sn2–O3	98.78 (8)
C1–Sn1–Cl1	96.22 (7)	C19–Sn2–O3	97.37 (8)
O1–Sn1–Cl1	162.37 (5)	O1–Sn2–O3	147.28 (6)
O3–Sn3–C31	117.32 (8)	O3–Sn4–C37	120.43 (8)

O3–Sn3–O4	73.40 (6)	O3–Sn4–C43	119.40 (8)
C31–Sn3–O4	98.12 (8)	C37–Sn4–C43	119.45 (9)
O3–Sn3–C25	117.89 (8)	O3–Sn4–O4	73.00 (6)
C31–Sn3–C25	124.79 (9)	C37–Sn4–O4	93.08 (8)
O4–Sn3–C25	97.20 (8)	C43–Sn4–O4	95.57 (8)
O3–Sn3–O2	73.90 (6)	O3–Sn4–Cl2	87.37 (5)
C31–Sn3–O2	98.00 (8)	C37–Sn4–Cl2	94.97 (7)
O4–Sn3–O2	147.27 (6)	C43–Sn4–Cl2	96.12 (7)
C25–Sn3–O2	96.66 (8)	O4–Sn4–Cl2	160.23 (5)

Table 4. Selected bond lengths (Å) for polymorph **1**.

Atom–Atom	Bond length	Atom–Atom	Bond length
Sn1–O2	2.0170 (16)	Sn3–O3	2.0449 (15)
Sn1–C7	2.121 (2)	Sn3–C31	2.105 (2)
Sn1–C1	2.125 (2)	Sn3–O4	2.1125 (17)
Sn1–O1	2.1466 (16)	Sn3–C25	2.118 (2)
Sn1–Cl1	2.4468 (6)	Sn3–O2	2.1301 (15)
Sn2–O2	2.0424 (15)	Sn4–O3	2.0121 (16)
Sn2–C13	2.116 (2)	Sn4–C37	2.112 (2)
Sn2–C19	2.117 (2)	Sn4–C43	2.124 (2)
Sn2–O1	2.1252 (16)	Sn4–O4	2.1610 (16)
Sn2–O3	2.1277 (15)	Sn4–Cl2	2.4532 (6)

The sum of the angles about the hydroxide bridging μ_2-(O4) atom which three electron pairs are shared with two Sn(IV) atoms, of 360.01° (see Table 2 for details) evidences a flattening that is consistent with a trigonal planar arrangement around this atom. On the contrary, the sum of the angles about the hydroxide bridging μ_2-(O1) atom

for which three electron pairs are shared with two Sn(IV) atoms, of 349.49° (Table 2) reveals a distorted trigonal pyramidal arrangement. This pyramidal geometry at μ_2-(O1) atom is presumably due to its involvement in a C–H···O interaction (see Table 5 for details) which may cause a disturbance of the occurring throttling within the structure. The trigonal pyramidal geometry described at μ_2-(O1) is furthermore highlighted by the r.m.s deviation of 0.100 Å for the H1Sn1Sn2O1 plane. The r.m.s deviation for H4Sn2Sn3O4 of 0.005 Å, also confirms the trigonal planar geometry forehead described. The Sn(IV) centers are five-coordinated adopting a trigonal bipyramidal (tbp) like-arrangement exhibiting two different chemical environments: $Sn(C_6H_5)_2ClO(OH)$ for the two pairs of exocyclic Sn(IV) centers and $Sn(C_6H_5)_2O_2(OH)$ for the central Sn_2O_2 core [28-32]. For Sn(1) exocyclic atom of the chemical $Sn(C_6H_5)_2ClO(OH)$, the tbp basal plane is defined by C(1), C(7), and O(2), while the axial positions are occupied by hydroxide O(1) and chlorine Cl(1) atoms forming an angle of 162.37(5)° (Table 3), showing a deviation from a linear geometry [28-32]. For Sn(4) exocyclic atom of the same chemical $Sn(C_6H_5)_2ClO(OH)$, the tbp basal plane is defined by C(37), C(43), and O(3), while the axial positions are occupied by O(4) and Cl(2) atoms forming an angle of 160.23(5)° (Table 3), also showing a deviation from a linear geometry [28-32]. For Sn(2) and Sn(3) of the latter chemical $Sn(C_6H_5)_2O_2(OH)$, tbp basal planes are defined by C(13), C(19), and O(2), and C(25), C(31), and O(3), respectively. The apical sites of the tbp with Sn(2) are occupied by O(1) and O(3) atoms forming an angle of 147.28(6)° (Table 3) evidencing a deviation from linearity too [28-32]. For Sn(3) tbp, the apical sites are occupied by O(2) and O(4) atoms forming an angle of 147.27(6)° (Table 3) which likewise describes a deviation from linearity [28-32]. Furthermore, each μ_3-O atom (O2 and O3) edge-shares two equatorial positions and one apical site of three tbp, explaining the throttling (Figure 2).

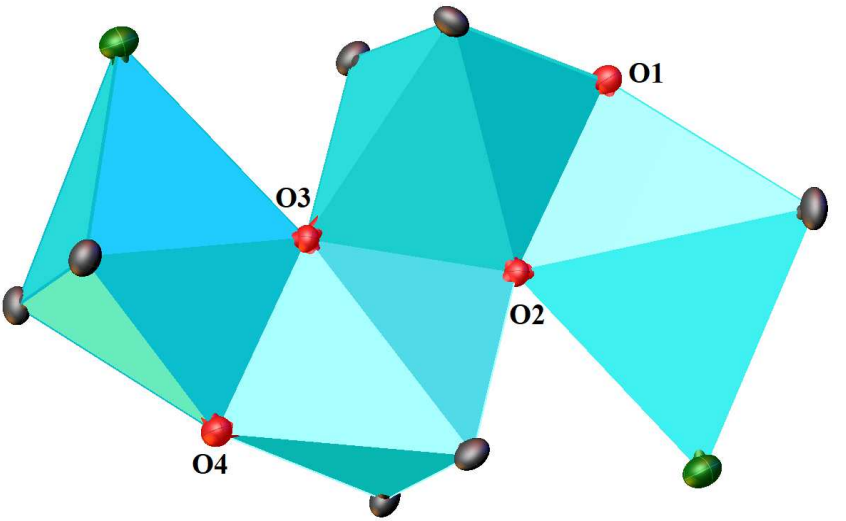

Figure 2. Molecular view of **1** showing 50% probability ellipsoids for atoms and the tbp polyhedra [atom color code: C, black; H, magenta; N, blue; O, red; Cl, green]. Only the carbon atoms linked to tin(IV) atoms are represented.

Although the sums of the angles about the endocyclic Sn(IV) centers of 359.9° (Sn2) and 360° (Sn3) (Table 3) evidence a planarity between these atoms and those defining basal planes of $Sn(C_6H_5)_2O_2(OH)$ tbp, the sums of the angles at exocyclic atoms Sn1 of 358.85° and Sn4 of 359.28° (Table 3) argue that these latter are slightly out the $Sn(C_6H_5)_2ClO(OH)$ relative tbp basal planes. The Tiekink's polymorph [28] exhibits a Sn···Sn separation of 3.3617(9) Å while this second polymorph shows shorter Sn···Sn separations as follows: Sn1···Sn2 of 3.3338(6) Å, Sn2···Sn3 of 3.3337(6) Å and Sn3···Sn4 of 3.3380(6) Å. The known polymorph reveals dihedral angles between the central Sn_2O_2 core and phenyl ring planes from 61.8(3) to 76.9(3)° in comparison to those from 60.87(10) to 78.06(10)° described in this work. The dihedral angles between the exocyclic Sn_2O_2 cores with phenyl ring planes vary from 55.27(10) to 80.22(10)°. Compared to the first polymorph reported by Tiekink which exhibits an almost perfect planar ladder with dihedral angles between the four-membered rings of 0.92(16)° [28], in this polymorph, the central Sn_2O_2 core forms dihedral angles of 4.00(7)° and 1.62(8)° with the two other external four-membered rings Sn_2O_2 units which form a dihedral angle of 4.65(8)°. These angles evidence a slightly bent ladder highlighting the deformation noticed. The lengthening of the hydroxide bridging Sn–O bonds (see Figure 3 and Table 4) is owing to a sequential transmission of static *trans* effect along the backbone.

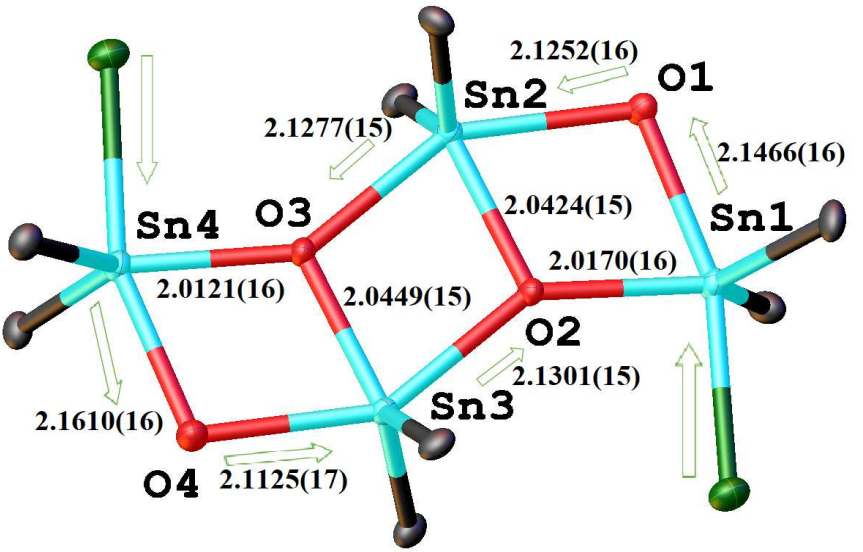

Figure 3. Molecular view of **1** showing 50% probability ellipsoids for atoms, the transmission way within tbp arrangements and the formed length distances [atom color code: C, black; H, magenta; N, blue; O, red; Cl, green; Sn, turquoise]. Only the carbon atoms linked to tin(IV) atoms are represented.

The higher *trans* effect of chloride compared to hydroxide strained the *trans* located μ_2-O atom, which therefore binds more strongly to the other Sn center (Figure 3 and Table 4) [28-32]. Due to the comparable static *trans* effect between hydroxide μ_2-O and oxide μ_3-O, the apical Sn–O bonds are almost similar (see Figure 3 and Table 4). The oxide μ_3-O bridging Sn–O bonds liable to a static *trans* effect from 2.1277(15) to 2.1301(15) Å are longer than those not liable, which all describe very close Sn–O bond values varying form 2.0121(16) to 2.0449(15) Å (Figure 3). These bond values also compare well with those found in earlier reported structures [28-32]. The Sn–C bond lengths from 2.105(2) to 2.125(2) Å are in accordance with the previously reported values for diphenyltin containing compounds [28-32, 45, 46]. Intermolecular O–H···O hydrogen bonds, involving the bridging hydroxyl group afford to connect the discrete tetranuclear organostannoxane ladder to neighboring DMF molecules which form a dihedral angle of 74.5(2)° (Figure 4). Closely inspecting the geometric parameters, a most detailed comparison with the first known polymorph and very close related structures is proposed (see Table 6).

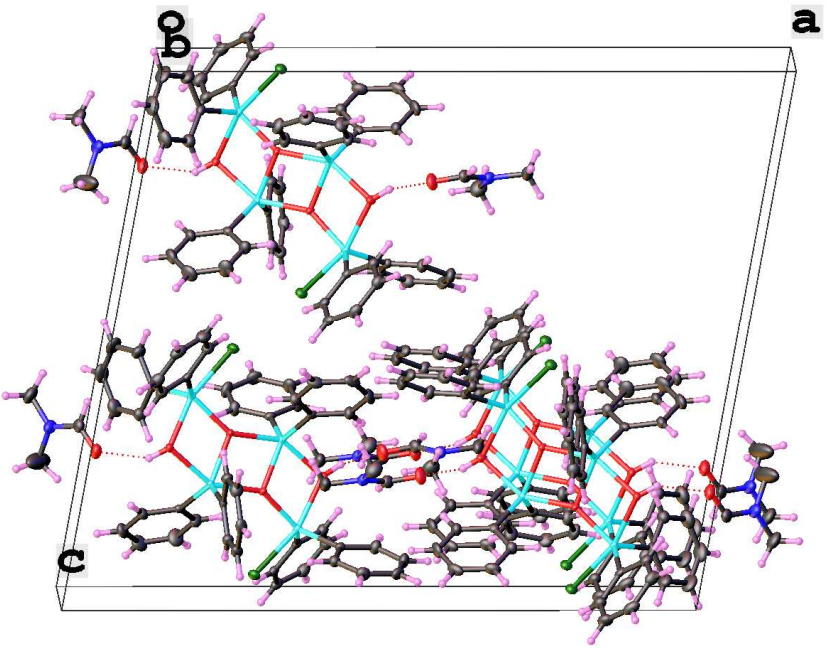

Figure 4. Partial packing diagram of **1** showing 50% probability ellipsoids for atoms, the hydrogen bonding linkage between the species and the arrangement of the molecules within the lattice [atom color code: C, black; H, magenta; N, blue; O, red; Cl, green; Sn, turquoise].

Intramolecular C–H···Cl and C–H···O hydrogen bonds, as well C–H···O interactions are present (see Table 5 for details). Moreover, the intermolecular C–H···O hydrogen bonds do not contribute to direct the crystal structure framework; they do not play an important function in forming a supramolecular architecture. Despite the weak hydrogen bonding patterns, the overall framework is arranged within the lattice (Figure 4) as previously encountered in the literature for the first polymorph and related structures [28-32].

Close inspection of crystal structure from PLATON [47] using KPI (Kitaigorodskii packing index) function revealed a higher value for packing index of 69.4% in comparison to the Tiekink's which afford a value of 65.9%.

Table 5. Prominent hydrogen bond and interaction geometries (Å, °) in the crystal structure of polymorph 1 [symmetry code: (i) $-x$, $y-1/2$, $-z+3/2$].

D–H···*A*	*d*(*D*–H)	*d*(H···*A*)	*d*(*D*···*A*)	∠(*D*–H···*A*)
O1–H1···O5	0.84	1.97	2.710(3)	146
O4–H4···O6	0.84	1.90	2.702(3)	160
C2–H2···O1	0.95	2.53	3.089(3)	118
C6–H6···Cl1	0.95	2.73	3.382(2)	126
C9–H9···O5^{i}	0.95	2.46	3.381(4)	165
C18–H18···Cl2	0.95	2.66	3.439(2)	140
C48–H48···Cl2	0.95	2.70	3.348(2)	126
C51–H51A···O5	0.98	2.38	2.768(5)	103
C53–H53A···O6	0.98	2.40	2.810(4)	105

Table 6. A comparison of the prominent geometric parameters within the second polymorph (**1**), the first polymorph and related structures containing the same organotin(IV) ladder and different molecule solvates.

CSD code [Reference]	**Compound 1 [This work]**	**JIGJAK [28]**	**CIJJEK [31]**	**LERQEG [32]**
Solvate	DMF	DMF	Acetone	DMSO
Crystal system	Monoclinic	Orthorhombic	Monoclinic	Monoclinic
Space group	$P2_1/c$ (n° 14)	Pbca (n° 61)	$P2_1/n$ (n° 14)	$P2_1/n$ (n° 14)
β/°	100.461(2)	-	92.87(1)	93.61(3)
Z/Z’	4/1	4/0.5	2/0.5	2/0.5
Presence of an inversion center	No	Yes	Yes	Yes
Sums of angles at μ_3-O	359.46° 359.95°	359.982°	359.636°	359.526°

Geometry at μ_3-O	Trigonal planar	Trigonal planar	Trigonal planar	Trigonal planar
Sums of angles at μ_2-O	349.49° 360.01°	359.594°	341.157°	330.582°
μ_2-O to trigonal basal plane distance	0.2423(17) 0.0132(18)	0.053(4)	0.37504(5)	0.42(2)
Geometry at μ_2-O	Trigonal planar and Trigonal pyramidal	Trigonal planar	Trigonal pyramidal	Trigonal pyramidal
Dihedral angles between central and external Sn_2O_2 rings	4.00(7)° 1.62(8)°	0.92(16)°	3.49°	3.62(9)°
Dihedral angles between external Sn_2O_2 rings	4.65(8)°	0.00(16)°	0.03°	0.00(9)°
Dihedral angles between phenyls of endocyclic Sn and central Sn_2O_2 ring	60.87(10)° 62.25(10)° 62.46(11)° 78.06(10)°	62.2(3)° 62.8(3)°	62.04° 66.92°	63.40(13)° 66.30(14)°
Dihedral angles between phenyls of exocyclic Sn and external Sn_2O_2 rings	55.27(10)° 58.93(11)° 72.72(12)° 76.14(11)°	64.9(3)° 76.9(3)°	57.28° 70.15°	55.79(14)° 68.47(13)°
Ladder's	Slightly bent	Planar	Slightly bent	Slightly bent

fashion				
Sums of angles at exocyclic Sn(IV)	358.85° 359.28°	359.569°	359.156°	359.312°
Exocyclic Sn(IV) to tbp basal plane distance	0.1300(13) 0.1023(13)	0.079(3)	0.111348(13)	0.1006(15)
Sums of angles at endocyclic Sn(IV)	359.9° 360°	359.759°	359.833°	359.927°
Endocyclic Sn(IV) to tbp basal plane distance	0.0371(13) 0.0013(14)	0.059(3)	0.049650(7)	0.0326(13)
Geometry at Sn(IV)	Tbp	tbp	tbp	tbp
Axial ∠(O–Sn–O)	147.28 (6)° 147.27 (6)°	146.009°	148.115°	148.272°
Axial ∠(O–Sn–Cl)	162.37 (5)° 160.23 (5)°	159.044°	159.991°	160.167°
Shorter and longer Sn–O bond	2.0121(16) 2.1610(16)	2.022 2.150	2.024 2.213	2.027 2.196

4. Conclusion

The tetranuclear organotin(IV) ladder, bis-[chloro-(μ_2-hydroxo)-(μ_3-oxo)-tetraphenyl-di-tin] present in this study, grown in a hydrolysis reaction of diphenyltin(IV) dichloride, has been found forming a co-crystalline 1:2 assembly with

dimethylformamide in a methanol mixed solvent when the reaction is carried out at room temperature under a non-controlled atmosphere. Its crystal structure investigated by single crystal X-ray diffraction analysis describes it to be the second polymorph of bis-[chloro-(μ_2-hydroxo)-(μ_3-oxo)-tetraphenyl-di-tin] dimethylformamide solvate. A comparison with the first polymorph and closely related tetranuclear organotin(IV) ladder complexes has shown similarities and slight differences. The geometry at oxygen O atoms within the ladder are almost all trigonal planar except one hydroxide bridging whose geometry is trigonal pyramidal. Crystals of compound **1** exhibits an overall framework arranged within the lattice while some hydrogen bonds are present. Further works in the area of organotin(IV) organostannoxanes are in progress.

5. Conflicts of Interest

There are no conflicts to declare.

6. Acknowledgement

The authors gratefully acknowledge the Cheikh Anta Diop University (Senegal) and the University of Notre Dame (USA) for equipment facilities.

References

[1] Hoti, N., Zhu, D.E., Song, Z., Wu, Z., Tabassum, S., & Wu, M. (2004). P53-dependent apoptotic mechanism of a new designer bimetallic compound tri-phenyl tin benzimidazolethiol copper chloride (TPT-CuCl2): In vivo studies in Wistar rats as well as in vitro studies in human cervical cancer cells. *Journal of Pharmacology and Experimental Therapeutics*, *311*, 22-33.https://doi.org/10.1124/jpet.104.069104

[2] Wang, S., Li, Q.-L., Zhang, R.-F., Du, J.-Y., Li, Y.-X., & Ma, C.-L. (2019). Novel organotin(IV) complexes derived from 4-carboxybenzenesulfonamide: Synthesis, structure and in vitro cytostatic activity evaluation. *Polyhedron*, *158*, 15-24. https://doi.org/10.1016/j.poly.2018.10.048

[3] Person, R.J., & Whalen, M.M. (2010). Effects of butyltin exposures on MAP kinase-dependent transcription regulators in human natural killer cells. *Toxicology Mechanisms and Methods*, *20*, 227-233. https://doi.org/10.3109/15376511003746034

[4] Carraher, C., Roner, M., Lynch, M., Moric-Johnson, A., Miller, L., Slawek, P., Mosca, F., & Frank, J. (2018). Organotinpoly(ester ethers) from salicylic acid and their ability to

inhibit human cancer cell lines. *Journal of Clinical Research in Oncology*, *1*(1), 1-11. https://doi.org/10.33309/2639-8230.010103

[5] Syed Annuar, S.N., Kamaludin, N.F., Awang, N., & Chan, K.M. (2021). Cellular basis of organotin(IV) derivatives as anticancer metallodrugs: a review. *Frontiers in Chemistry*, *9*, 657599. https://doi.org/10.3389/fchem.2021.657599

[6] Carraher, Jr., C. (2017). *Introduction to polymer chemistry* (4th ed.). NY: CRC Press; Taylor and Francis. https://doi.org/10.1201/9781315369488

[7] Etaiw, S.E.H., Abd El-Aziz, D.M., & Ali, E.A. (2019). Crystal structure, cytotoxicity and biological activity of hydrogen bonded networks based on dimethyltin (IV) and bipodal ligands. *Journal of Organometallic Chemistry*, *894*, 43-60. https://doi.org/10.1016/j.jorganchem.2019.05.007

[8] Devendra, R., Edmonds, N.R., & Sohnel, T. (2015). Organotin carboxylate catalyst in urethane formation in a polar solvent: an experimental and computational study. *RSC Advances*, *5*, 48935-48945. https://doi.org/10.1039/C5RA03367E

[9] Carraher, C.E., Roner, M.R., Miller, L., Shahi, K., Trang, N.T., Moric-Johnson, A., Barot, G., Battin, A., & Alhuniti, M.H. (2014). Control of colorectal cancer using organotin polymers. *Journal of the Chinese Advanced Materials Society*, *2*, 303-325. http://dx.doi.org/10.1080/22243682.2014.966274

[10] Diop, T., Diop, M.B., Diop, C.A.K., Diassé-Sarr, A., Sidibé, M., Dumitru, F., & van der Lee, A. (2022). Synthesis and structural characterization of new ladder-like organostannoxanes derived from carboxylic acid derivatives: $[C_5H_4N(p\text{-}CO_2)]_2[Bu_2Sn]_4(\mu_3\text{-}O)_2(\mu_2\text{-}OH)_2$, $[Ph_2CHCO_2]_4[Bu_2Sn]_4(\mu_3\text{-}O)_2$, and $[(p\text{-}NH_2)\text{-}C_6H_4\text{-}CO_2]_2[Bu_2Sn]_4(\mu_3\text{-}O)_2(\mu_2\text{-}OH)_2$. *Main Group Metal Chemistry*, *45*, 1-9. https://doi.org/10.1515/mgmc-2022-0008

[11] Banti, C.N., Hadjikakou, S.K., Sismanoglu, T., & Hadjiliadis, N. (2019). Antiproliferative and antitumor activity of organotin(IV) compounds. An overview of the last decade and future perspectives. *Journal of Inorganic Biochemistry*, *194*, 114-152. https://doi.org/10.1016/j.jinorgbio.2019.02.003

[12] Arjmand, F., Parveen, S., Tabassum, S., & Pettinari, C. (2014). Organotin antitumor compounds: their present status in drug development and future perspectives. *Inorganica Chimica Acta*, *423*, 26-37.https://doi.org/10.1016/j.ica.2014.07.066

[13] Wang, Q.F., Ma, C.L., He, G.F., & Li, Z. (2013). Synthesis and characterization of new tin derivatives derived from 3,5,6-trichlorosalicylic acid: Cage, chain and ladder X-ray crystal structures. *Polyhedron*, *49*, 177-182.https://doi.org/10.1016/j.poly.2012.09.057

[14] García-Zarracino, R., Höpfl, H., & Rodríguez, M.G. (2009). Bis(tetraorganodistannoxanes) as secondary building block units (SBUs) for the generation of porous materials − A three-dimensional honeycomb architecture containing adamantane-type water clusters. *Crystal Growth & Design*, *9*, 1651-1654. https://doi.org/10.1021/cg801313u

[15] Beckmann, J., Jurkschat, J., Rabe, K., Schürmann, M., & Dakternieks, D. (2001). New insights in asymmetric tetraorganodistannoxane ladder formation. A NMR-spectroscopic and crystallographic study. *Zeitschrift für Anorganische und Allgemeine Chemie*, *627*, 458-464. https://doi.org/10.1002/1521-3749(200103)627:3<458::AID-ZAAC458>3.0.CO;2-N

[16] Wen, G-H., Zhang, R-F., Li, Q-L., Zhang, S-L., Ru, J., Du, J-Y., & Ma, C.L. (2018). Synthesis, structure and in vitro cytostatic activity study of the novel organotin(IV) derivatives of p-aminobenzenesulfonic acid. *Journal of Organometallic Chemistry*, *861*, 151-158. https://doi.org/10.1016/j.jorganchem.2018.02.033

[17] Balas, V.I., Banti, C.N., Kourkoumelis, N., Hadjikakou, S.K., Geromichalos, G.D., Sahpazidou, D., Male, L., Hursthouse, M.B., Bednarz, B., Kubicki, M., Charalabopoulos, K., & Hadjiliadis, N. (2012). Structural and in vitro biological studies of organotin(IV) precursors; selective inhibitory activity against human breast cancer cells, positive to estrogen receptors. *Australian Journal of Chemistry*, *65*, 1625-1637. https://doi.org/10.1071/CH12448

[18] Kresinski, R.A., Staples, R.J., & Fackler Jnr, J.P. (1994). Structure of dichlorobis(μ-hydroxo)bis(μ$_3$-oxo)octaphenyltetratin(IV), $[Sn_4Cl_2(O)_2(OH)_2(C_6H_5)_8]$. *Acta Crystallographica*, *C50*, 40-41. https://doi.org/10.1107/S0108270193006018

[19] Cox, M.J., & Tiekink, E.R.T. (1994). Crystal structure of bis[chloro-1kCl-μ-hydroxo-μ-oxo-(tetraphenyl-1K^{2}C,2K^{2}C)ditin], $[Cl(C_6H_5)_2Sn(OH)OSn(C_6H_5)_2]_2$. *Z. Krist. Crystallogr*, *209*, 622-623. https://doi.org/10.1524/zkri.1994.209.7.622

[20] Barba, V., Vega, E., Luna, R., Hopfl, H., Beltran, H.I., & Zamudio-Rivera, L.S. (2007). Structural and conformational analysis of neutral dinucleardiorganotin(IV) complexes derived from hexadentate Schiff base ligands. *Journal of Organometallic Chemistry*, *692*, 731-739. https://doi.org/10.1016/j.jorganchem.2006.09.064

[21] Yap, Q.L., Lo, K.M., & Ng, S.W. (2010). Dibromidodi-μ-hydroxido-di-μ$_3$-oxido-octaphenyltetratin(IV). *Acta Crystallographica*, *E66*, m8. https://doi.org/10.1107/S1600536809051691

[22] Puff, H., Bung, I., Friedrichs, E., & Jansen, A. (1983). Kristallstrukturen von isopropyl-undtrimethylsilylmethylen-substituiertenchloro-hydroxo-tetraorganyl-distannoxanen. *Journal of Organometallic Chemistry*, *254*, 23-32. https://doi.org/10.1016/0022-328X(83)85113-4

[23] Zhang, Q.-J., Yin, H.-D., Wen, L.-Y., & Wang, D.-Q. (2009). Dichloridooctakis(2-chlorobenzyl)di-μ_2-hydroxido-di-μ_3-oxido-tetratin(IV). *Acta Crystallographica*, *E65*, m1494. https://doi.org/10.1107/S1600536809045176

[24] Momeni, B.Z., Fathi, N., Moghadasi, M., Biglari, A., & Janczak, J. (2019). New insight into the reactions of organoplatinum(II) complexes with diorganotin dichloride and diisothiocyanate: Oxidative addition, reductive elimination and α-elimination. *Journal of Organometallic Chemistry*, *880*, 368-377. https://doi.org/10.1016/j.jorganchem.2018.11.022

[25] Zhang, F.-X., Wang, J.-Q., Kuang, D.-Z., Feng, Y.-L., Zhang, Z.-J., Xu, Z.-F., & He, P. (2009). Synthesis, crystal structure and quantum chemistry of the ladder bis(p-methylbenzyl)tin oxo(chlo) cluste. *Chinese Journal of Inorganic Chemistry*, *25*, 1812-1817.

[26] Wang, Y.-H., Ye, Z.-J., Jin, X.-H., Yao, J.-H., Chen N.-H., & Zhu D.-S. (2007). Synthesis, characterize and crystal structure of di-μ_2-hydroxy-dichloro-bis-μ_3-oxy-octa-benzyl-tetratin. *Journal of Northeast Normal University Natural Science Edition*, *39*, 90-93.

[27] Baumeister, U., Dakternieks, D., Jurkschat, K., & Schürmann, M. (2002). A rare example of an unsymmetrically substituted tetraorganodistannoxane ladder: [cyclo-Hex_2(OH)SnOSn(Cl)t-Bu_2]$_2$. *Main Group Metal Chemistry*, *25*, 521-522. https://doi.org/10.1515/MGMC.2002.25.8.521

[28] Tiekink, E.R.T. (1991). A dimericstannoxane structure: [Sn_2(Cl)(O)(OH)(C_6H_5)$_4$]$_2$.2C_3H_7NO. *Acta Crystallographica*, *C47*, 661-662. https://doi.org/10.1107/S0108270190009787

[29] Mohamed, E.M., Panchanatheswaran, K., Low, J.N., & Glidewell, C. (2004). Octa-benzyldichlorodi-μ_2-hydroxo-di-μ_3-oxo-tetratin toluene disolvate. *Acta Crystallographica*, *E60*, m489-m491. https://doi.org/10.1107/S160053680400697X

[30] Lo, K.M., & Ng, S.W. (2009). Dichloridooctakis(4-chlorobenzyl)di-μ_2-hydroxido-di-μ_3-oxido-tetratin(IV) toluene solvate. *Acta Crystallographica*, *E65*, m593. https://doi.org/10.1107/S1600536809015128

[31] Vollano, J.F., Day, R.O., & Holmes, R.R. (1984). Pentacoordinated molecules. 54. Hydrolysis pathway leading to the formation of novel oxo- and halo-bridged tin(IV) ladder compounds. The molecular structure of the dimericdistannoxanes [Ph_2(Cl)SnOSnPh_2(OH)]$_2$.cntdot.2Me_2CO and [Ph_2(Cl)SnOSnPh_2(Cl)]$_2$. *Organometallics*, *3*, 745-750. https://doi.org/10.1021/om00083a017

[32] Foladi, S., Khazaei, P., Gharamaleki, J.A., Notash, B., & Rofouei, M.K. (2013). Dichloridodi-μ_2-hydroxido-di-μ_3-oxido-octa-phenyl-tetra-tin(IV) dimethyl sulfoxide disolvate. *Acta Crystallographica*, *E69*, m91. https://doi.org/10.1107/S1600536812051744

[33] Diop, T., Ndiolene, A., Diop, M.B., Boye, M.S., van der Lee, A., Dumitru, F., Diop, C.A.K., & Sidibé, M. (2021). Synthesis, spectral (FT-IR, ^{1}H, ^{13}C) studies and crystal structure of $[(2,6\text{-}CO_2)_2C_5H_3NSnBu_2(H_2O)]_2{\cdot}CHCl_3$. *Zeitschrift für Naturforschung*, *B76*, 127-132. https://doi.org/10.1515/znb-2020-0195

[34] Diop, M.B., Seck, G. A., Sarr, M.,Diop, L., & Oliver, A.G. (2020). Co-crystallization of oxalate salts of monoprotonated amines with a double Sn-Ph bond cleavage. *American Journal of Heterocyclic Chemistry*, *6*, 16-23. https://doi.org/10.11648/j.ajhc.20200602.11

[35] Sarr, M., Diop, M.B., Diassé-Sarr, A., Wang, A., & Englert, U. (2020). Crystal structure of triphenyltin(IV) formate polymer, $(HCO_2SnPh_3)_n$. *Journal of Engineering Studies and Research*, *26*, 212-217. https://doi.org/10.29081/jesr.v26i3.226

[36] Diop, M.B., Diop, L., Plasseraud, L., & Cattey, H. (2016). Triorganotin carboxylates – synthesis and crystal structure of 2-methyl-1*H*-imidazol-3-ium *catena*-*O*,*O'*-oxalatotriphenylstannate. *Main Group Metal Chemistry*, *39*, 119-123. https://doi.org/10.1515/mgmc-2016-0016

[37] Diop, M.B., Diop, L., & Oliver, A.G. (2016). Crystal structure of bis(2-methyl-1H-imidazol-3-ium) μ-oxalato-bis[n-butyltrichloridostannate(IV)]. *Acta Crystallographica*, *E72*, 858-860.https://doi.org/10.1107/S2056989016008434

[38] Gueye, N., Diop, L., Molloy, K.C., & Kociok-Kohn, G. (2011). Crystal structure of $C_2O_4(SnPh_3{\cdot}\text{dimethylformamide})_2$. *Main Group Metal Chemistry*, *34*, 3-4. https://doi.org/10.1515/mgmc.2011.008

[39] Apex3 (2017). Area Detector Integration Software, Bruker AXS Inc.: Madison, Wisconsin (USA).

[40] SAINT (2017). Data Reduction and Frame Integration Program for the CCD Area-Detector System, Bruker AXS Inc.: Madison, Wisconsin (USA).

[41] Krause, L., Herbst-Irmer, R., Sheldrick, G.M., & Stalke, D. (2015). Comparison of silver and molybdenum microfocus X-ray sources for single-crystal structure determination. *Journal of Applied Crystallography*, *48*, 3-10. https://doi.org/10.1107/S1600576714022985

[42] Sheldrick, G.M. (2015). SHELXT-Integrated space-group and crystal structure determination. *Acta Crystallographica*, *A71*(1), 3-8. https://doi.org/10.1107/S2053273314026370

[43] Sheldrick, G.M. (2015). Crystal structure refinement with SHELXL. *Acta Crystallographica*, *C71*(1), 3-8. https://doi.org/10.1107/S2053229614024218

[44] Dolomanov, O.V., Bourhis, L.J., Gildea, R.J., Howard, J.A.K., & Puschmann, H. (2009).

OLEX2: a complete structure solution, refinement and analysis program. *Journal of Applied Crystallography*, *42*(2), 339-341. https://doi.org/10.1107/S0021889808042726

[45] Al-Shakban, M., Matthews, P.D., Lewis, E.A., Raftery, J., Vitorica-Yrezabal, I, Haigh, S.J., Lewis, D.J., & O'Brien, P. (2019). Chemical vapor deposition of tin sulfide from diorganotin(IV) dixanthates. *Journal of Materials Science*, *54*, 2315-2323. https://doi.org/10.1007/s10853-018-2968-y

[46] Haezam, F.N., Awang, N., Kamaludin, N.F., Jotani, M.M., & Tiekink, E.R.T. (2020). (*N*,*N*-Diallyldithiocarbamato-κ^2*S*,*S*′)triphenyltin(IV) and bis(*N*,*N*-diallyldithiocarbamato-κ^2*S*,*S*′)diphenyltin(IV): crystal structure, Hirshfeld surface analysis and computational study. *Acta Crystallographica*, *E76*, 167-176. https://doi.org/10.1107/S2056989020000122

[47] Spek, A.L. (2009). Structure validation in chemical crystallography. *Acta Crystallographica*, *D65*, 148-155. https://doi.org/10.1107/S090744490804362X